

Backward Stability of Explicit External Deflation for the Symmetric Eigenvalue Problem

Chao-Ping Lin*

Ding Lu†

Zhaojun Bai‡

May 5, 2021

Abstract

A thorough backward stability analysis of Hotelling’s deflation, an explicit external deflation procedure through low-rank updates for computing many eigenpairs of a symmetric matrix, is presented. Computable upper bounds of the loss of the orthogonality of the computed eigenvectors and the symmetric backward error norm of the computed eigenpairs are derived. Sufficient conditions for the backward stability of the explicit external deflation procedure are revealed. Based on these theoretical results, the strategy for achieving numerical backward stability by dynamically selecting the shifts is proposed. Numerical results are presented to corroborate the theoretical analysis and to demonstrate the stability of the procedure for computing many eigenpairs of large symmetric matrices arising from applications.

1 Introduction

Let A be an $n \times n$ real symmetric matrix with ordered eigenvalues $\lambda_1 \leq \lambda_2 \leq \dots \leq \lambda_n$, and the corresponding eigenvectors v_1, v_2, \dots, v_n . Let $\mathcal{I} = [\lambda_{\text{low}}, \lambda_{\text{upper}}]$ be an interval containing the eigenvalues $\lambda_1, \lambda_2, \dots, \lambda_{n_e}$ at the lower end of the spectrum of A . We are interested in computing the partial eigenvalue decomposition

$$AV_{n_e} = V_{n_e}\Lambda_{n_e}, \quad (1.1)$$

where $\Lambda_{n_e} = \text{diag}(\lambda_1, \lambda_2, \dots, \lambda_{n_e})$, $V_{n_e} = [v_1, v_2, \dots, v_{n_e}]$ and $V_{n_e}^T V_{n_e} = I_{n_e}$. We are particularly interested in the case where the interval is of the width $|\mathcal{I}| = \lambda_{\text{upper}} - \lambda_{\text{low}} \leq \frac{1}{2}\|A\|_2$, and may contain a large number of eigenvalues of A .

A majority of subspace projection methods for computing the partial eigenvalue decomposition (1.1), such as the Lanczos methods [13, 1], typically converge first to the eigenvalues on the periphery of the spectrum. A projection subspace of a large dimension is necessary to compute the eigenvalues located deep inside the spectrum. Maintaining the orthogonality of a large projection subspace is computationally expensive. To reduce the dimensions of projection subspaces and accelerate the convergence, a number of techniques such as the restarting [17, 8, 20] and the filtering [11] have been developed.

This paper revisits a classical deflation technique known as Hotelling’s deflation [6, 19, 13]. Hotelling’s deflation computes the partial eigenvalue decomposition (1.1) through a sequence of low-rank updates. In the simplest case, supposing that the lowest eigenpair (λ_1, v_1) of A is computed

*Department of Mathematics, University of California, Davis, CA 95616, USA, cplin@ucdavis.edu

†Department of Mathematics, University of Kentucky, Lexington, KY 40506, USA, Ding.Lu@uky.edu

‡Department of Mathematics and Department of Computer Science, University of California, Davis, CA 95616, USA, zbai@ucdavis.edu

by an eigensolver, by choosing a real shift σ_1 and defining the rank-one update matrix

$$A_1 \equiv A + \sigma_1 v_1 v_1^T,$$

the eigenpair (λ_1, v_1) of A is displaced to an eigenpair $(\lambda_1 + \sigma_1, v_1)$ of A_1 , while all the other eigenpairs of A and A_1 are the same. If the shift $\sigma_1 > \lambda_{\text{upper}} - \lambda_1$, then the eigenpair (λ_1, v_1) is shifted outside the interval \mathcal{I} and the eigenpair (λ_2, v_2) of A becomes the lowest eigenpair of A_1 . Subsequently, we can use the eigensolver again to compute the lowest eigenpair (λ_2, v_2) of A_1 . The procedure is repeated until all the eigenvalues in the interval \mathcal{I} are found. Since the low-rank update of the original A can be done outside of the eigensolver, we refer to this strategy as an explicit external deflation (EED) procedure, to distinguish from the deflation techniques used inside an eigensolver, such as TRLan [20] and ARPACK [9]. Recently the EED has been combined with Krylov subspace methods to progressively compute the eigenpairs toward the interior of the spectrum of symmetric eigenvalue problems [12, 21], and extended to structured eigenvalue problems [2, 3].

In the presence of finite precision arithmetic, the EED procedure is susceptible to numerical instability due to the accumulation of numerical errors from previous computations; see, e.g., [19, p. 585] and [15, p. 96]. In [13, Chap. 5.1], Parlett showed that the change to the smallest eigenvalue in magnitude by deflating out the largest computed eigenvalue would be at the same order of the round-off error incurred. In [14], for nonsymmetric matrices, Saad derived an upper bound on the backward error norm and showed that the stability is determined by the angle between the computed eigenvectors and the deflated subspace. Saad concluded that “if the angle between the computed eigenvector and the previous invariant subspace is small at every step, the process may quickly become unstable. On the other hand, if this is not the case then the process is quite safe, for small number of requested eigenvalues.”

However, none of the existing studies had examined the effect of the choice of shifts on the numerical stability. In this paper, we present a thorough backward stability analysis of the EED procedure. We first derive governing equations of the EED procedure in the presence of finite precision arithmetic, and then derive upper bounds of the loss of the orthogonality of the computed eigenvectors and the symmetric backward error norm of the computed eigenpairs. From these upper bounds, under mild assumptions, we conclude that the EED procedure is backward stable if the shifts σ_j are dynamically chosen such that (i) the spectral gaps, defined as the separation between the computed eigenvalues and shifted ones, are maintained at the same order of the norm of the matrix A , and (ii) the shift-gap ratios, defined as the ratios between the largest shift in magnitude and the spectral gaps, are at the order of one. Our analysis implies that the re-orthogonalization of computed eigenvectors and the large angles between the computed eigenvectors and the previous invariant subspaces are unnecessary. Based on theoretical analysis, we provide a practical shift selection scheme to guarantee the backward stability. For a set of test matrices from applications, we demonstrate that the EED in combination with an established eigensolver can compute a large number of eigenvalues with backward stability.

The rest of the paper is organized as follows. In Section 2, we present the governing equations of the EED in finite precision arithmetic. In Section 3, we derive the upper bounds on the loss of orthogonality of computed eigenvectors and the symmetric backward error norm of computed eigenpairs. From these upper bounds, we derive conditions for the backward stability of the EED procedure. In Section 4, we discuss how to properly choose the shifts to satisfy the stability conditions and outline an algorithm for combining the EED procedure with an eigensolver. Numerical results to verify the sharpness of the upper bounds and to demonstrate the backward stability of the EED for symmetric eigenvalue problems from applications are presented in Section 5. Concluding remarks are given in section 6.

Following the convention of matrix computations, we use the upper case letters for matrices and the lower case letters for vectors. In particular, we use I_n for the identity matrix of dimension n . If not specified, the dimensions of matrices and vectors conform to the dimensions used in the context. We use \cdot^T for transpose, and $\|\cdot\|_2$ and $\|\cdot\|_F$ for 2-norm and the Frobenius norm, respectively. The range of a matrix A is denoted by $\mathcal{R}(A)$. We also use $\sigma_{\min}(\cdot)$ to denote the minimal singular values of a matrix. Other notations will be explained as used.

2 EED in finite precision arithmetic

Suppose that we use an established eigensolver called EIGSOL, such as TRLan [20] and ARPACK [9], to successfully compute the lowest eigenpair $(\widehat{\lambda}, \widehat{v})$ of A with

$$A\widehat{v} = \widehat{\lambda}\widehat{v} + \eta,$$

where $\|\widehat{v}\|_2 = 1$ and the residual vector η satisfies

$$\|\eta\|_2 \leq \text{tol} \cdot \|A\|_2 \quad (2.1)$$

for a prescribed convergence tolerance tol . The EED procedure starts with computing the lowest eigenpair $(\widehat{\lambda}_1, \widehat{v}_1)$ of A by EIGSOL satisfying

$$A\widehat{v}_1 = \widehat{\lambda}_1\widehat{v}_1 + \eta_1,$$

where $\widehat{\lambda}_1 \in \mathcal{I} = [\lambda_{\text{low}}, \lambda_{\text{upper}}]$, and the residual vector η_1 satisfies (2.1). At the first EED step, we choose a shift σ_1 and define

$$\widehat{A}_1 \equiv A + \sigma_1\widehat{v}_1\widehat{v}_1^T.$$

By choosing the shift $\sigma_1 > \lambda_{\text{upper}} - \widehat{\lambda}_1$, the lowest eigenpair of \widehat{A}_1 is an approximation of the second eigenpair (λ_2, v_2) of A . Subsequently, we use EIGSOL to compute the lowest eigenpair $(\widehat{\lambda}_2, \widehat{v}_2)$ of \widehat{A}_1 satisfying

$$\widehat{A}_1\widehat{v}_2 = \widehat{\lambda}_2\widehat{v}_2 + \eta_2,$$

where the residual vector η_2 satisfies (2.1). Meanwhile, expressing the computed eigenpair $(\widehat{\lambda}_1, \widehat{v}_1)$ in terms of \widehat{A}_1 , we have

$$\widehat{A}_1\widehat{v}_1 = (\widehat{\lambda}_1 + \sigma_1)\widehat{v}_1 + \eta_1.$$

Proceeding to the second EED step, we choose a shift σ_2 and define

$$\widehat{A}_2 \equiv \widehat{A}_1 + \sigma_2\widehat{v}_2\widehat{v}_2^T = A + \widehat{V}_2\Sigma_2\widehat{V}_2^T,$$

where $\widehat{V}_2 = [\widehat{v}_1, \widehat{v}_2]$ and $\Sigma_2 = \text{diag}(\sigma_1, \sigma_2)$. By choosing the shift $\sigma_2 > \lambda_{\text{upper}} - \widehat{\lambda}_2$, the lowest eigenpair of \widehat{A}_2 is an approximation of the third eigenpair (λ_3, v_3) of A . Then we use EIGSOL again to compute the lowest eigenpair $(\widehat{\lambda}_3, \widehat{v}_3)$ of \widehat{A}_2 satisfying

$$\widehat{A}_2\widehat{v}_3 = \widehat{\lambda}_3\widehat{v}_3 + \eta_3,$$

where the residual vector η_3 satisfies (2.1). Meanwhile, expressing the computed eigenpairs $(\widehat{\lambda}_1, \widehat{v}_1)$ and $(\widehat{\lambda}_2, \widehat{v}_2)$ in terms of \widehat{A}_2 , we have

$$\widehat{A}_2\widehat{V}_2 = \widehat{V}_2(\widehat{\Lambda}_2 + \Sigma_2) + \widehat{V}_2\Sigma_2\Phi_2 + E_2,$$

where $\widehat{\Lambda}_2 = \text{diag}(\widehat{\lambda}_1, \widehat{\lambda}_2)$, $E_2 = [\eta_1, \eta_2]$, and $\Phi_2 \in \mathbb{R}^{2 \times 2}$ is the strictly lower triangular part of the matrix $\widehat{V}_2^T \widehat{V}_2 - I_2$, i.e., $\Phi_2 + \Phi_2^T = \widehat{V}_2^T \widehat{V}_2 - I_2$.

In general, at the j -th EED step, we choose a shift σ_j and define

$$\widehat{A}_j \equiv \widehat{A}_{j-1} + \sigma_j \widehat{v}_j \widehat{v}_j^T = A + \widehat{V}_j \Sigma_j \widehat{V}_j^T, \quad (2.2)$$

where $\widehat{V}_j \equiv [\widehat{v}_1, \dots, \widehat{v}_j]$ and $\Sigma_j = \text{diag}(\sigma_1, \dots, \sigma_j)$ with $\widehat{A}_0 \equiv A$. Then by choosing the shift $\sigma_j > \lambda_{\text{upper}} - \widehat{\lambda}_j$, the lowest eigenpair of \widehat{A}_j is an approximation of the $(j+1)$ -th eigenpair (λ_{j+1}, v_{j+1}) of A . We use EIGSOL to compute the lowest eigenpair $(\widehat{\lambda}_{j+1}, \widehat{v}_{j+1})$ of \widehat{A}_j satisfying

$$\widehat{A}_j \widehat{v}_{j+1} = \widehat{\lambda}_{j+1} \widehat{v}_{j+1} + \eta_{j+1}, \quad (2.3)$$

where $\|\widehat{v}_{j+1}\|_2 = 1$ and the residual vector η_{j+1} satisfies (2.1), i.e.,

$$\|\eta_{j+1}\|_2 \leq \text{tol} \cdot \|A\|_2. \quad (2.4)$$

Meanwhile, for the computed eigenpairs $(\widehat{\lambda}_j, \widehat{v}_j)$ in terms of \widehat{A}_j , we have

$$\widehat{A}_j \widehat{v}_j = \widehat{A}_{j-1} \widehat{v}_j + \sigma_j \widehat{v}_j = (\lambda_j + \sigma_j) \widehat{v}_j + \eta_j, \quad (2.5)$$

and for the computed eigenpairs $(\widehat{\lambda}_i, \widehat{v}_i)$ with $1 \leq i \leq j-1$ in terms of \widehat{A}_j , we have

$$\begin{aligned} \widehat{A}_j \widehat{v}_i &= \left(\widehat{A}_{j-1} + \sigma_j \widehat{v}_j \widehat{v}_j^T \right) \widehat{v}_i \\ &= \left(\widehat{A}_{i-1} + \sigma_i \widehat{v}_i \widehat{v}_i^T + \widehat{V}_{i+1:j} \Sigma_{i+1:j} \widehat{V}_{i+1:j}^T \right) \widehat{v}_i \\ &= \left(\widehat{A}_{i-1} + \sigma_i \widehat{v}_i \widehat{v}_i^T \right) \widehat{v}_i + \widehat{V}_{i+1:j} \Sigma_{i+1:j} \widehat{V}_{i+1:j}^T \widehat{v}_i \\ &= \widehat{\lambda}_i \widehat{v}_i + \eta_i + \sigma_i \widehat{v}_i + \widehat{V}_{i+1:j} \Sigma_{i+1:j} \widehat{V}_{i+1:j}^T \widehat{v}_i \\ &= (\widehat{\lambda}_i + \sigma_i) \widehat{v}_i + \widehat{V}_{i+1:j} \Sigma_{i+1:j} \widehat{V}_{i+1:j}^T \widehat{v}_i + \eta_i \\ &= (\widehat{\lambda}_i + \sigma_i) \widehat{v}_i + \widehat{V}_j \Sigma_j \begin{bmatrix} 0 \\ \widehat{V}_{i+1:j}^T \widehat{v}_i \end{bmatrix} + \eta_i, \end{aligned} \quad (2.6)$$

where $\widehat{V}_{i+1:j} \equiv [\widehat{v}_{i+1}, \dots, \widehat{v}_j]$ and $\Sigma_{i+1:j} \equiv \text{diag}(\sigma_{i+1}, \dots, \sigma_j)$.

Combining (2.5) and (2.6), we have

$$\widehat{A}_j \widehat{V}_j = \widehat{V}_j (\widehat{\Lambda}_j + \Sigma_j) + \widehat{V}_j \Sigma_j \Phi_j + E_j, \quad (2.7)$$

where $\widehat{\Lambda}_j = \text{diag}(\widehat{\lambda}_1, \dots, \widehat{\lambda}_j)$, $E_j = [\eta_1, \dots, \eta_j]$, Φ_j is the strictly lower triangular part of the matrix $\widehat{V}_j^T \widehat{V}_j - I_j$ and $\Phi_j + \Phi_j^T = \widehat{V}_j^T \widehat{V}_j - I_j$. Eqs. (2.3) and (2.7) are referred to as *the governing equations of j steps of (inexact) EED procedure*.

For the backward stability analysis of the EED procedure, we introduce the following two quantities associated with the shifts $\sigma_1, \dots, \sigma_j$ for a j -step EED:

- the *spectral gap* of \widehat{A}_j , defined as the separation between the computed eigenvalues and the shifted ones:

$$\gamma_j \equiv \min_{\lambda \in \mathcal{I}_{j+1}, \theta \in \mathcal{J}_j} |\lambda - \theta| > 0, \quad (2.8)$$

where $\mathcal{I}_{j+1} \equiv \{\widehat{\lambda}_1, \dots, \widehat{\lambda}_j, \widehat{\lambda}_{j+1}\}$, the set of computed eigenvalues, and $\mathcal{J}_j \equiv \{\widehat{\lambda}_1 + \sigma_1, \dots, \widehat{\lambda}_j + \sigma_j\}$, the set of computed eigenvalues after shifting (see Figure 1 for an illustration);

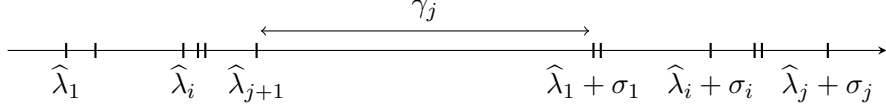


Figure 1: Illustration of the spectral gap γ_j

- the *shift-gap ratio*, defined as the ratio of the largest shift and the spectral gap γ_j :

$$\tau_j \equiv \frac{1}{\gamma_j} \cdot \max_{1 \leq i \leq j} |\sigma_i|. \quad (2.9)$$

We will see that γ_j and τ_j are crucial quantities to characterize the backward stability of the EED procedure.

3 Backward stability analysis of EED

In this section, we first review the notion of backward stability for the computed eigenpairs. Then we derive upper bounds on the loss of orthogonality of computed eigenvectors and the backward error norm of computed eigenpairs by the EED procedure, and reveal conditions for the backward stability of the procedure.

3.1 Notion of backward stability

By the well-established notion of backward stability analysis in numerical linear algebra [5, 18], the following two quantities measure the accuracy of the approximate eigenpairs $(\hat{\Lambda}_{j+1}, \hat{V}_{j+1})$ of A computed by the EED procedure:

- the loss of orthogonality of the computed eigenvectors \hat{V}_{j+1} ,

$$\omega_{j+1} \equiv \|\hat{V}_{j+1}^T \hat{V}_{j+1} - I_{j+1}\|_F, \quad (3.1)$$

- the symmetric backward error norm of the computed eigenpairs $(\hat{\Lambda}_{j+1}, \hat{V}_{j+1})$,

$$\delta_{j+1} \equiv \min_{\Delta \in \mathcal{H}_{Q_{j+1}}} \|\Delta\|_F, \quad (3.2)$$

where $\mathcal{H}_{Q_{j+1}}$ is the set of the symmetric backward errors for the orthonormal basis Q_{j+1} from the polar decomposition¹ of \hat{V}_{j+1} , namely,

$$\mathcal{H}_{Q_{j+1}} \equiv \left\{ \Delta \mid (A + \Delta)Q_{j+1} = Q_{j+1}\hat{\Lambda}_{j+1}, \Delta = \Delta^T \in \mathbb{R}^{n \times n} \right\}. \quad (3.3)$$

For a prescribed tolerance tol of the stopping criterion (2.4) for an eigensolver EIGSOL, the EED procedure is considered to be *backward stable* if

$$\omega_{j+1} = O(tol) \quad (3.4)$$

and

$$\delta_{j+1} = O(tol \cdot \|A\|_2), \quad (3.5)$$

where the constants in the big-O notations are low-degree polynomials in the number j of the EED steps.

¹The polar decomposition of a matrix X is given by $X = UP$ where U is orthonormal and P is symmetric positive semi-definite.

3.2 Loss of orthogonality

We first prove the following lemma to reveal the structure of the orthogonality between the computed eigenvectors.

Lemma 3.1. *By the governing equations (2.3) and (2.7) of j steps of EED, if $\tau_j \omega_j < \sqrt{2}$, then for $i = 1, 2, \dots, j$, the matrices $\Gamma_i \equiv \widehat{\Lambda}_i + \Sigma_i - \widehat{\lambda}_{i+1} I_i$ and $I_i + \Phi_i^T \Sigma_i \Gamma_i^{-1}$ are non-singular, and*

$$\widehat{V}_i^T \widehat{v}_{i+1} = \Gamma_i^{-1} (I_i + \Phi_i^T \Sigma_i \Gamma_i^{-1})^{-1} \left[\widehat{V}_i^T \eta_{i+1} - E_i^T \widehat{v}_{i+1} \right]. \quad (3.6)$$

Furthermore,

$$(i) \quad \|\Gamma_i^{-1}\|_2 \leq \gamma_j^{-1},$$

$$(ii) \quad \|(I_i + \Phi_i^T \Sigma_i \Gamma_i^{-1})^{-1}\|_2 \leq (1 - \tau_j \omega_j / \sqrt{2})^{-1},$$

where γ_j and τ_j are the spectral gap and the shift-gap ratio defined in (2.8) and (2.9), respectively, and ω_j is the loss of the orthogonality defined in (3.1).

Proof. By the governing equations (2.3) and (2.7) of j steps of EED, for $1 \leq i \leq j$, we have

$$\widehat{V}_i^T \widehat{A}_i \widehat{v}_{i+1} = \widehat{\lambda}_{i+1} \widehat{V}_i^T \widehat{v}_{i+1} + \widehat{V}_i^T \eta_{i+1}$$

and

$$\widehat{V}_i^T \widehat{A}_i \widehat{v}_{i+1} = (\widehat{\Lambda}_i + \Sigma_i) \widehat{V}_i^T \widehat{v}_{i+1} + \Phi_i^T \Sigma_i \widehat{V}_i^T \widehat{v}_{i+1} + E_i^T \widehat{v}_{i+1}.$$

Consequently,

$$(\Gamma_i + \Phi_i^T \Sigma_i) \widehat{V}_i^T \widehat{v}_{i+1} = \widehat{V}_i^T \eta_{i+1} - E_i^T \widehat{v}_{i+1}, \quad (3.7)$$

where $\Gamma_i = \widehat{\Lambda}_i + \Sigma_i - \widehat{\lambda}_{i+1} I_i$ is a diagonal matrix.

By the definition (2.8) of the spectral gap γ_j ,

$$\sigma_{\min}(\Gamma_i) = \min_{1 \leq k \leq i} |\widehat{\lambda}_k + \sigma_k - \widehat{\lambda}_{i+1}| \geq \gamma_j > 0. \quad (3.8)$$

Hence the matrix Γ_i is non-singular and the bound (i) holds.

Since Φ_i is the strictly lower triangular part of the matrix $\widehat{V}_i^T \widehat{V}_i - I_i$,

$$\|\Phi_i^T\|_2 \leq \|\Phi_i^T\|_F = \frac{\omega_i}{\sqrt{2}} \leq \frac{\omega_j}{\sqrt{2}}.$$

Consequently,

$$\|\Phi_i^T \Sigma_i \Gamma_i^{-1}\|_2 \leq \|\Phi_i^T\|_2 \|\Gamma_i^{-1}\|_2 \|\Sigma_i\|_2 \leq \frac{\omega_j}{\sqrt{2}} \cdot \gamma_j^{-1} \cdot \|\Sigma_j\|_2 = \frac{\omega_j}{\sqrt{2}} \cdot \tau_j < 1, \quad (3.9)$$

where for the last inequality, we use the assumption $\tau_j \omega_j < \sqrt{2}$. By (3.9), the matrix $I_i + \Phi_i^T \Sigma_i \Gamma_i^{-1}$ is non-singular and the bound (ii) holds due to $\|(I + X)^{-1}\|_2 \leq (1 - \|X\|_2)^{-1}$ for any X with $\|X\|_2 < 1$.

Since both matrices Γ_i and $I_i + \Phi_i^T \Sigma_i \Gamma_i^{-1}$ are invertible, the identity (3.6) follows from (3.7). \square

Next we exploit the structure of the product $\widehat{V}_i^T \widehat{v}_{i+1}$ to derive a computable upper bound on the loss of orthogonality ω_{j+1} of computed eigenvectors \widehat{V}_{j+1} .

Theorem 3.1. *By the governing equations (2.3) and (2.7) of j steps of EED, if $\tau_j \omega_j < \sqrt{2}$, then the loss of orthogonality ω_{j+1} of the computed eigenvectors \widehat{V}_{j+1} defined in (3.1) satisfies*

$$\omega_{j+1} \leq 2 \frac{c_j}{\gamma_j} \left(1 + 2 \frac{c_j}{\gamma_j} \|E_{j+1}\|_{\mathbb{F}} \right) \|E_{j+1}\|_{\mathbb{F}}, \quad (3.10)$$

where $c_j = (1 - \tau_j \omega_j / \sqrt{2})^{-1}$, and γ_j and τ_j are the spectral gap and the shift-gap ratio defined in (2.8) and (2.9), respectively.

Proof. By the definition (3.1), we have

$$\omega_{j+1}^2 = 2 \cdot \|\Phi_{j+1}^{\mathbb{T}}\|_{\mathbb{F}}^2 = 2 \cdot \sum_{i=1}^j \|\widehat{V}_i^{\mathbb{T}} \widehat{v}_{i+1}\|_2^2. \quad (3.11)$$

Recall Lemma 3.1 that, for any $1 \leq i \leq j$,

$$\|\widehat{V}_i^{\mathbb{T}} \widehat{v}_{i+1}\|_2 \leq \frac{c_j}{\gamma_j} \cdot \|\widehat{V}_i^{\mathbb{T}} \eta_{i+1} - E_i^{\mathbb{T}} \widehat{v}_{i+1}\|_2.$$

Hence we can derive from (3.11) that

$$\begin{aligned} \omega_{j+1}^2 &\leq \frac{2c_j^2}{\gamma_j^2} \cdot \sum_{i=1}^j \|\widehat{V}_i^{\mathbb{T}} \eta_{i+1} - E_i^{\mathbb{T}} \widehat{v}_{i+1}\|_2^2 \\ &= \frac{2c_j^2}{\gamma_j^2} \cdot \frac{1}{2} \|\widehat{V}_{j+1}^{\mathbb{T}} E_{j+1} - E_{j+1}^{\mathbb{T}} \widehat{V}_{j+1}\|_{\mathbb{F}}^2 \\ &\leq \frac{2c_j^2}{\gamma_j^2} \cdot 2 \|\widehat{V}_{j+1}^{\mathbb{T}} E_{j+1}\|_{\mathbb{F}}^2 \leq \frac{4c_j^2}{\gamma_j^2} \cdot \|\widehat{V}_{j+1}^{\mathbb{T}}\|_2^2 \|E_{j+1}\|_{\mathbb{F}}^2. \end{aligned} \quad (3.12)$$

Since

$$\|\widehat{V}_{j+1}^{\mathbb{T}}\|_2^2 = \|\widehat{V}_{j+1}^{\mathbb{T}} \widehat{V}_{j+1}\|_2 \leq \|I_{j+1}\|_2 + \|\widehat{V}_{j+1}^{\mathbb{T}} \widehat{V}_{j+1} - I_{j+1}\|_2 \leq 1 + \omega_{j+1},$$

we arrive at

$$\omega_{j+1}^2 \leq \frac{4c_j^2}{\gamma_j^2} \cdot (1 + \omega_{j+1}) \cdot \|E_{j+1}\|_{\mathbb{F}}^2. \quad (3.13)$$

Letting $t = \omega_{j+1} / \chi_{j+1}$, where $\chi_{j+1} = 2c_j \|E_{j+1}\|_{\mathbb{F}} / \gamma_j$, then the inequality (3.13) is recast as

$$t^2 - \chi_{j+1} t - 1 \leq 0. \quad (3.14)$$

By the fact that the quadratic polynomial in (3.14) is concave, we conclude that

$$t \leq \frac{1}{2} \cdot \left(\chi_{j+1} + \sqrt{4 + \chi_{j+1}^2} \right) \leq \frac{1}{2} \cdot (\chi_{j+1} + 2 + \chi_{j+1}) \leq 1 + \chi_{j+1}.$$

This proves the upper bound in (3.10). \square

Remark 3.1. A straightforward way to derive an upper bound of ω_{j+1} is to use the relation

$$\omega_{j+1}^2 = \omega_j^2 + 2 \cdot \|\widehat{V}_j^{\mathbb{T}} \widehat{v}_{j+1}\|_2^2,$$

and the following bound from Lemma 3.1

$$\|\widehat{V}_j^T \widehat{v}_{j+1}\|_2^2 \leq \frac{c_j^2}{\gamma_j^2} \cdot \left(\|\widehat{V}_j\|_2 \|\eta_{j+1}\|_2 + \|E_j\|_F \right)^2 \approx \frac{c_j^2}{\gamma_j^2} (\|E_{j+1}\|_F^2 + 2\|\eta_{j+1}\|_2 \|E_j\|_F).$$

However, this would lead to a pessimistic upper bound of ω_{j+1} . In contrast, in Theorem 3.1, we exploit the structure of the orthogonality $\widehat{V}_i^T \widehat{v}_{i+1}$ to obtain a tighter bound (3.10) of ω_{j+1} . Eq. (3.12) in the proof is the key step. In Example 5.1 in Section 5, we will demonstrate numerically that the bound (3.10) is indeed a tight upper bound on the loss of orthogonality ω_{j+1} .

3.3 Symmetric backward error norm

In this section, we derive a computable upper bound on the symmetric backward error norm δ_{j+1} of computed eigenpairs $(\widehat{\Lambda}_{j+1}, \widehat{V}_{j+1})$ of A defined in (3.2). First, the following lemma gives an upper bound of the norm of the residual for $(\widehat{\Lambda}_{j+1}, \widehat{V}_{j+1})$:

$$R_{j+1} \equiv A\widehat{V}_{j+1} - \widehat{V}_{j+1}\widehat{\Lambda}_{j+1}. \quad (3.15)$$

Lemma 3.2. *By the governing equations (2.3) and (2.7) of j steps of EED, if $\tau_j \omega_j < \sqrt{2}$, then for the computed eigenpairs $(\widehat{\Lambda}_{j+1}, \widehat{V}_{j+1})$ of A , the Frobenius norm of the residual R_{j+1} defined in (3.15) satisfies*

$$\|R_{j+1}\|_F \leq \left(1 + \sqrt{2}c_j \tau_j (1 + \omega_{j+1})\right) \|E_{j+1}\|_F, \quad (3.16)$$

where $c_j = (1 - \tau_j \omega_j / \sqrt{2})^{-1}$, and γ_j and τ_j are the spectral gap and the shift-gap ratio defined in (2.8) and (2.9), respectively.

Proof. From the governing equation (2.7) of the EED procedure after $j+1$ steps, we have

$$\widehat{A}_{j+1} \widehat{V}_{j+1} = \widehat{V}_{j+1} (\widehat{\Lambda}_{j+1} + \Sigma_{j+1}) + \widehat{V}_{j+1} \Sigma_{j+1} \Phi_{j+1} + E_{j+1}. \quad (3.17)$$

On the other hand, by the definition (2.2) of \widehat{A}_{j+1} , we have

$$\begin{aligned} \widehat{A}_{j+1} \widehat{V}_{j+1} &= A\widehat{V}_{j+1} + \widehat{V}_{j+1} \Sigma_{j+1} \widehat{V}_{j+1}^T \widehat{V}_{j+1} \\ &= A\widehat{V}_{j+1} + \widehat{V}_{j+1} \Sigma_{j+1} (\Phi_{j+1} + I_{j+1} + \Phi_{j+1}^T). \end{aligned} \quad (3.18)$$

Combining (3.17) and (3.18), we obtain the residual

$$R_{j+1} = A\widehat{V}_{j+1} - \widehat{V}_{j+1} \widehat{\Lambda}_{j+1} = E_{j+1} - \widehat{V}_{j+1} \Sigma_{j+1} \Phi_{j+1}^T. \quad (3.19)$$

Consequently, the norm of the residual R_{j+1} is bounded by

$$\|R_{j+1}\|_F \leq \|E_{j+1}\|_F + \|\widehat{V}_{j+1}\|_2 \|\Sigma_{j+1} \Phi_{j+1}^T\|_F. \quad (3.20)$$

Note that $\Sigma_{j+1} = \text{diag}(\sigma_1, \dots, \sigma_{j+1})$ and Φ_{j+1}^T is the strictly upper triangular part of the matrix $\widehat{V}_{j+1}^T \widehat{V}_{j+1} - I_{j+1}$, and we have

$$\begin{aligned} \|\widehat{V}_{j+1}\|_2 \|\Sigma_{j+1} \Phi_{j+1}^T\|_F &\leq \|\widehat{V}_{j+1}\|_2 \|\Sigma_j\|_2 \|\Phi_{j+1}^T\|_F \\ &\leq \|\widehat{V}_{j+1}\|_2 \|\Sigma_j\|_2 \cdot \frac{1}{\sqrt{2}} \omega_{j+1} \\ &\leq \frac{1}{\sqrt{2}} \|\Sigma_j\|_2 \sqrt{(1 + \omega_{j+1}) \omega_{j+1}^2}, \end{aligned} \quad (3.21)$$

where, for the third inequality, we again use the fact that $\|\widehat{V}_{j+1}\|_2 \leq \sqrt{1 + \omega_{j+1}}$ by the definition of the loss of orthogonality ω_{j+1} . Left-multiplying (3.13) by $1 + \omega_{j+1}$, we know that

$$(1 + \omega_{j+1})\omega_{j+1}^2 \leq \frac{4c_j^2}{\gamma_j^2} \cdot (1 + \omega_{j+1})^2 \cdot \|E_{j+1}\|_{\mathbb{F}}^2.$$

Plugging into (3.21), we obtain

$$\begin{aligned} \|\widehat{V}_{j+1}\|_2 \|\Sigma_{j+1} \Phi_{j+1}^T\|_{\mathbb{F}} &\leq \sqrt{2} \|\Sigma_j\|_2 c_j \gamma_j^{-1} \cdot (1 + \omega_{j+1}) \cdot \|E_{j+1}\|_{\mathbb{F}} \\ &= \sqrt{2} c_j \tau_j \cdot (1 + \omega_{j+1}) \cdot \|E_{j+1}\|_{\mathbb{F}}. \end{aligned}$$

Combine with (3.20) and we arrive at the upper bound (3.16) of $\|R_{j+1}\|_{\mathbb{F}}$. \square

Now we recall the following theorem by Sun [18].

Theorem 3.2 (Thm.3.1 in [18]). *Let (Λ, X) be approximate eigenpairs of a symmetric matrix A . Let Q be the orthonormal basis from the polar decomposition of X . Define the set*

$$\mathcal{H}_Q = \{\Delta \mid (A + \Delta)Q = Q\Lambda, \Delta = \Delta^T \in \mathbb{R}^{n \times n}\}. \quad (3.22)$$

Then \mathcal{H}_Q is non-empty and there exists a unique $\Delta_Q \in \mathcal{H}_Q$ such that

$$\min_{\Delta \in \mathcal{H}_Q} \|\Delta\|_{\mathbb{F}} = \|\Delta_Q\|_{\mathbb{F}} \leq \sqrt{\|R\|_{\mathbb{F}}^2 + \|\mathcal{P}_X^\perp R\|_{\mathbb{F}}^2} / \sigma_{\min}(X), \quad (3.23)$$

where $R = AX - X\Lambda$ is the residual and \mathcal{P}_X^\perp is the orthogonal projection onto the orthogonal complement of $\mathcal{R}(X)$.

From Lemma 3.2 and Theorem 3.2, we have the following computable upper bound on the symmetric backward error norm δ_{j+1} of the computed eigenpairs $(\widehat{\Lambda}_{j+1}, \widehat{V}_{j+1})$ of A .

Theorem 3.3. *By the governing equations (2.3) and (2.7) of j steps of EED, if $\tau_j \omega_j < \sqrt{2}$ and $\omega_{j+1} < 1$, then the symmetric backward error norm δ_{j+1} of the computed eigenpairs $(\widehat{\Lambda}_{j+1}, \widehat{V}_{j+1})$ of A defined in (3.2) has the following upper bound*

$$\delta_{j+1} \leq \sqrt{2} \left(\frac{1 + c_j \tau_j (1 + \omega_{j+1})}{\sqrt{1 - \omega_{j+1}}} \right) \|E_{j+1}\|_{\mathbb{F}}, \quad (3.24)$$

where $c_j = (1 - \tau_j \omega_j / \sqrt{2})^{-1}$, and γ_j and τ_j are the spectral gap and the shift-gap ratio defined in (2.8) and (2.9), respectively.

Proof. For the computed eigenvectors \widehat{V}_{j+1} of A , let Q_{j+1} be the orthonormal basis from the polar decomposition of \widehat{V}_{j+1} , and the set $\mathcal{H}_{Q_{j+1}}$ be defined in (3.3). It follows from the definition (3.2) and Theorem 3.2 that

$$\delta_{j+1} = \min_{\Delta \in \mathcal{H}_{Q_{j+1}}} \|\Delta\|_{\mathbb{F}} \leq \frac{1}{\sigma_{\min}(\widehat{V}_{j+1})} \sqrt{\|R_{j+1}\|_{\mathbb{F}}^2 + \|\mathcal{P}^\perp R_{j+1}\|_{\mathbb{F}}^2}, \quad (3.25)$$

where R_{j+1} is the residual of $(\widehat{\Lambda}_{j+1}, \widehat{V}_{j+1})$ defined in (3.15), and \mathcal{P}^\perp is the orthogonal projection onto the orthogonal complement of the subspace $\mathcal{R}(\widehat{V}_{j+1})$, i.e.,

$$\mathcal{P}^\perp = I - \widehat{V}_{j+1} (\widehat{V}_{j+1}^T \widehat{V}_{j+1})^{-1} \widehat{V}_{j+1}^T.$$

By the equation (3.19), $\mathcal{P}^\perp R_{j+1} = \mathcal{P}^\perp E_{j+1}$. Hence we have

$$\|\mathcal{P}^\perp R_{j+1}\|_F = \|\mathcal{P}^\perp E_{j+1}\|_F \leq \|E_{j+1}\|_F. \quad (3.26)$$

On the other hand, by the definition (3.1) of ω_{j+1} and the assumption $\omega_{j+1} < 1$, we have

$$|\sigma_{\min}^2(\widehat{V}_{j+1}) - 1| \leq \|\widehat{V}_{j+1}^T \widehat{V}_{j+1} - I_{j+1}\|_2 \leq \omega_{j+1} < 1,$$

which implies the following lower bound of the singular value

$$\sigma_{\min}(\widehat{V}_{j+1}) \geq \sqrt{1 - \omega_{j+1}}. \quad (3.27)$$

Plug (3.26) and (3.27) into (3.25) and recall the upper bound of $\|R_{j+1}\|_F$ in Lemma 3.2, and then we obtain

$$\begin{aligned} \delta_{j+1} &\leq \sqrt{1 + \left(1 + \sqrt{2}c_j\tau_j \cdot (1 + \omega_{j+1})\right)^2} \cdot \frac{\|E_{j+1}\|_F}{\sqrt{1 - \omega_{j+1}}} \\ &\leq \sqrt{2} \left(\frac{1 + c_j\tau_j(1 + \omega_{j+1})}{\sqrt{1 - \omega_{j+1}}} \right) \|E_{j+1}\|_F, \end{aligned}$$

where the second inequality is due to $1 + (1 + \sqrt{2}a)^2 \leq 2(1 + 2a + a^2) = 2(1 + a)^2$. This completes the proof. \square

Remark 3.2. We note from the inequalities (3.25) and (3.27) that, when $\omega_{j+1} \ll 1$, the residual norm $\|R_{j+1}\|_F$ can be used as an easy-to-compute estimate of δ_{j+1} . We will use this observation in numerical examples in Section 5.

3.4 Backward stability of EED

In Theorems 3.1 and 3.3, the upper bounds (3.10) and (3.24) for δ_{j+1} and ω_{j+1} involve the quantity ω_j from the previous EED step. In this section, under a mild assumption, we derive explicit upper bounds for ω_{j+1} and δ_{j+1} , and then reveal conditions for the backward stability of the EED procedure.

Lemma 3.3. *Consider j steps of EED governed by Eqs. (2.3) and (2.7). Assume*

$$\tau_j \frac{\|A\|_2}{\gamma_j} \cdot 4\sqrt{j+1} \cdot \text{tol} < 0.1. \quad (3.28)$$

Then

(i) *it holds that*

$$\tau_i \omega_i < 0.11 \quad \text{and} \quad c_i = (1 - \tau_i \omega_i / \sqrt{2})^{-1} < 2 \quad \text{for } i = 1, 2, \dots, j; \quad (3.29)$$

(ii) *the loss of orthogonality ω_{j+1} is bounded by*

$$\omega_{j+1} \leq \left(\frac{\|A\|_2}{\gamma_j} \cdot 5\sqrt{j+1} \right) \cdot \text{tol}; \quad (3.30)$$

(iii) *the backward error norm δ_{j+1} is bounded by*

$$\delta_{j+1} \leq \left(\tau_j \cdot 5\sqrt{j+1} \right) \cdot \text{tol} \cdot \|A\|_2. \quad (3.31)$$

Proof. First observe that by the definitions (2.8) and (2.9), γ_i is monotonically decreasing with the index i and $\tau_i \geq 1$ is monotonically increasing with i . Therefore, the assumption (3.28) implies the inequalities

$$\frac{\|A\|_2}{\gamma_i} \cdot 4\sqrt{i+1} \cdot \text{tol} < 0.1 \quad \text{and} \quad \tau_i \frac{\|A\|_2}{\gamma_{i-1}} \cdot 4\sqrt{i} \cdot \text{tol} < 0.1 \quad \text{for all } i \leq j. \quad (3.32)$$

Since the stopping criterion (2.4) of EIGSOL implies

$$\|E_i\|_F = \|\eta_1, \dots, \eta_i\|_F \leq \sqrt{i} \cdot \text{tol} \cdot \|A\|_2, \quad (3.33)$$

inequalities (3.32) leads to

$$\frac{4}{\gamma_i} \cdot \|E_{i+1}\|_F < 0.1 \quad \text{and} \quad \tau_i \cdot \frac{4}{\gamma_{i-1}} \cdot \|E_i\|_F < 0.1 \quad \text{for all } i \leq j. \quad (3.34)$$

(i) We prove the inequality (3.29) by induction. To begin with, recall that $\|\widehat{v}_1\|_2 = 1$, which implies $\omega_1 = \|\widehat{v}_1^T \widehat{v}_1 - 1\|_F = 0$, $\tau_1 \omega_1 = 0 < 0.11$, and $c_1 = 1 < 2$. Hence (3.29) holds for $i = 1$. Now, for $2 \leq i \leq j$, assume that $\tau_{i-1} \omega_{i-1} < 0.11$ and $c_{i-1} < 2$. Since $\tau_{i-1} \omega_{i-1} < 0.11$, we can apply Theorem 3.1 and derive from (3.10) that

$$\tau_i \omega_i \leq \tau_i \cdot \frac{2c_{i-1}}{\gamma_{i-1}} \|E_i\|_F \cdot \left(1 + \frac{2c_{i-1}}{\gamma_{i-1}} \|E_i\|_F\right) < 0.1 \cdot (1 + 0.1) = 0.11, \quad (3.35)$$

where the last inequality of (3.35) is by $2c_{i-1} < 4$ and (3.34). This implies immediately

$$c_i = (1 - \tau_i \omega_i / \sqrt{2})^{-1} \leq (1 - 0.11 / \sqrt{2})^{-1} < 2.$$

Therefore, (3.29) follows by induction.

(ii) Since we have $\tau_j \omega_j < 0.11$ and $c_j < 2$ by (3.29), we can apply Theorem 3.1 and derive from (3.10) that

$$\omega_{j+1} \leq \frac{2c_j}{\gamma_j} \cdot \|E_{j+1}\|_F \cdot \left(1 + \frac{2c_j}{\gamma_j} \|E_{j+1}\|_F\right) \leq \frac{4}{\gamma_j} \cdot \|E_{j+1}\|_F \cdot (1 + 0.1), \quad (3.36)$$

where in the second inequality we used $2c_j < 4$ and the first inequality in (3.34). Recall the error bound of $\|E_{j+1}\|_F$ from (3.33) and we obtain (3.30).

(iii) We have $\tau_j \omega_j < 0.11$ and $c_j < 2$ by (3.29). It also follows from (3.36) and (3.34) that $\omega_{j+1} < 0.11$. Therefore, we can apply Theorem 3.3 and derive from (3.24) that

$$\delta_{j+1} \leq \sqrt{2} \left(\frac{1 + c_j \tau_j (1 + \omega_{j+1})}{\sqrt{1 - \omega_{j+1}}} \right) \|E_{j+1}\|_F \leq \sqrt{2} \left(\frac{1 + 2\tau_j (1 + 0.11)}{\sqrt{1 - 0.11}} \right) \cdot \|E_{j+1}\|_F,$$

where in second inequality we used $0 \leq \omega_{j+1} < 0.11$. Since $\tau_j \geq 1$ by definition (2.9), we can relax the leading constant as $\sqrt{2}(1.06 + 2.36 \cdot \tau_j) \leq \sqrt{2}(3.42 \cdot \tau_j) < 5\tau_j$. Recall the error bound of $\|E_{j+1}\|_F$ from (3.33) and we prove (3.31). \square

By the error bounds (3.30) and (3.31) in Lemma 3.3, we can see that the quantities $\gamma_j^{-1} \|A\|_2$ and τ_j play important roles for the stability of the EED procedure. A sufficient condition to achieve the backward stability (3.4) and (3.5) is given by $\gamma_j^{-1} \|A\|_2 = O(1)$ and $\tau_j = O(1)$. In summary, we have the following theorem for the backward stability of the EED procedure.

Theorem 3.4. *Under the assumptions of the residual norm $\|\eta_i\|_2$ of EIGSOL satisfying (2.1) and the inequality (3.28), the backward stability of the EED procedure, in the sense of (3.4) and (3.5), is guaranteed if the shifts $\sigma_1, \dots, \sigma_j$ are dynamically chosen such that*

$$\gamma_j^{-1}\|A\|_2 = O(1) \quad \text{and} \quad \tau_j = O(1). \quad (3.37)$$

We note that when the shifts σ_j are dynamically chosen such that the conditions (3.37) are satisfied, the assumption of the inequality (3.28) is indeed mild.

Remark 3.3. From the upper bound (3.30) of the loss of orthogonality ω_{j+1} , we see that if the spectral gap γ_j is too small, i.e., $\gamma_j \ll \|A\|_2$, then ω_{j+1} could be amplified by a factor of $\gamma_j^{-1}\|A\|_2$. On the other hand, from the upper bound (3.31) of the symmetric backward error norm δ_{j+1} , we see that when τ_j is too large, i.e., $\tau_j \gg 1$, δ_{j+1} could be amplified by a factor of τ_j . We will demonstrate these observations numerically in Example 5.2 in Section 5.

4 EED in practice

In Section 3.4, we derived the required conditions (3.37) of the spectral gap γ_j and the shift-gap ratio τ_j for the backward stability of the EED procedure. The quantities γ_j and τ_j are controlled by the selection of the shifts $\sigma_1, \dots, \sigma_j$. In this section, we discuss a practical selection scheme of the shifts to satisfy the conditions (3.37), and then present an algorithm that combines an eigensolver EIGSOL with the EED procedure to compute eigenvalues in a prescribed interval $\mathcal{I} = [\lambda_{\text{low}}, \lambda_{\text{upper}}]$.

4.1 Choice of the shifts

We consider the following choice of the shift at the j -th EED step,

$$\sigma_j = \mu - \widehat{\lambda}_j, \quad (4.1)$$

where $\mu \in \mathbb{R}$ is a parameter with $\mu > \lambda_{\text{upper}}$. The shifting scheme (4.1) has been used in several previous works, although without elaboration on the choice of parameter μ ; see [13, Chap.5.1] and [12, 21]. In the following, we will discuss how to choose the parameter μ such that the conditions (3.37) can hold.

To begin with, the choice of the shifts in (4.1) implies that the spectral gap γ_j in (2.8) satisfies

$$\gamma_j = \min_{\theta \in \mathcal{I}_{j+1}, \lambda \in \mathcal{J}_j} |\lambda - \theta| = \min_{1 \leq i \leq j+1} |\mu - \widehat{\lambda}_i|, \quad (4.2)$$

where $\mathcal{I}_{j+1} = \{\widehat{\lambda}_1, \dots, \widehat{\lambda}_j, \widehat{\lambda}_{j+1}\}$ and $\mathcal{J}_j = \{\widehat{\lambda}_1 + \sigma_1, \dots, \widehat{\lambda}_j + \sigma_j\} = \{\mu\}$. On the other hand, it also implies that the shift-gap ratio τ_j in (2.9) satisfies

$$\tau_j = \frac{1}{\gamma_j} \cdot \max_{1 \leq i \leq j} |\sigma_i| = \frac{\max_{1 \leq i \leq j} |\mu - \widehat{\lambda}_i|}{\min_{1 \leq i \leq j+1} |\mu - \widehat{\lambda}_i|}. \quad (4.3)$$

Now recall that $\mu > \lambda_{\text{upper}}$ and the computed eigenvalues $\widehat{\lambda}_i \in [\lambda_{\text{low}}, \lambda_{\text{upper}}]$, for $i = 1, 2, \dots, j+1$, so we have

$$\mu - \lambda_{\text{upper}} \leq \min_{1 \leq i \leq j+1} |\mu - \widehat{\lambda}_i| \leq \max_{1 \leq i \leq j+1} |\mu - \widehat{\lambda}_i| \leq \mu - \lambda_{\text{low}}.$$

Hence, (4.2) and (4.3) lead to

$$\gamma_g \leq \gamma_j \leq \gamma_g \tau_g \quad \text{and} \quad \tau_j \leq \tau_g, \quad (4.4)$$

where

$$\gamma_g \equiv \mu - \lambda_{\text{upper}} \quad \text{and} \quad \tau_g \equiv \frac{\mu - \lambda_{\text{low}}}{\mu - \lambda_{\text{upper}}}.$$

The problem is then turned to the choice of parameter μ such that the quantities γ_g and τ_g to satisfy the conditions (3.37).

Let us consider a frequently encountered case in practice where the width of the interval $\mathcal{I} = [\lambda_{\text{low}}, \lambda_{\text{upper}}]$ satisfies

$$\lambda_{\text{upper}} - \lambda_{\text{low}} \leq \frac{1}{2} \|A\|_2.$$

Then by setting

$$\mu = \widehat{\lambda}_1 + \|A\|_2,$$

we have

$$\frac{1}{2} \|A\|_2 \leq \gamma_g = \left(1 - \frac{\lambda_{\text{upper}} - \widehat{\lambda}_1}{\|A\|_2} \right) \|A\|_2 \leq \|A\|_2$$

and

$$\tau_g = 1 + \frac{\lambda_{\text{upper}} - \lambda_{\text{low}}}{\gamma_g} \leq 2.$$

Consequently, by (4.4), the spectral gap γ_j and the shift-gap ratio τ_j satisfy the desired conditions (3.37).

In summary, for the EED procedure in practice, we recommend the use of the following strategy for the choice of the shift σ_j at the j -th EED,

$$\sigma_j = \mu - \widehat{\lambda}_j \quad \text{with} \quad \mu = \widehat{\lambda}_1 + \|A\|_2, \quad (4.5)$$

to compute the eigenvalues in an interval $\mathcal{I} = [\lambda_{\text{low}}, \lambda_{\text{upper}}]$, where $\lambda_{\text{upper}} - \lambda_{\text{low}} \leq \frac{1}{2} \|A\|_2$.

4.2 Algorithm

An eigensolver EIGSOL combined with the EED procedure to compute the eigenvalues in an interval $\mathcal{I} = [\lambda_{\text{low}}, \lambda_{\text{upper}}]$ at the lower end of the spectrum of A is summarized in Algorithm 1.

Algorithm 1 An eigensolver EIGSOL combined with the EED procedure

Input: the interval $\mathcal{I} = [\lambda_{\text{low}}, \lambda_{\text{upper}}]$ at the lower end of the spectrum of A ; the relative tolerance tol in (2.1) for EIGSOL.

Output: the approximate eigenpairs $(\widehat{\lambda}_i, \widehat{v}_i)$ in the interval \mathcal{I} .

- 1: $\widehat{A}_0 = A$;
 - 2: use EIGSOL to compute the lowest eigenpair $(\widehat{\lambda}_1, \widehat{v}_1)$ of \widehat{A}_0 and an estimate **Anorm** of $\|A\|_2$;
 - 3: $\mu = \widehat{\lambda}_1 + \mathbf{Anorm}$;
 - 4: **for** $j = 1, 2, \dots$ **do**
 - 5: $\sigma_j = \mu - \widehat{\lambda}_j$;
 - 6: $\widehat{A}_j = \widehat{A}_{j-1} + \sigma_j \widehat{v}_j \widehat{v}_j^T = A + \widehat{V}_j \Sigma_j \widehat{V}_j^T$;
 - 7: compute the lowest eigenpair $(\widehat{\lambda}_{j+1}, \widehat{v}_{j+1})$ of \widehat{A}_j by EIGSOL;
 - 8: check if all the eigenpairs in the interval \mathcal{I} have been computed;
 - 9: **end for**
 - 10: return the approximate eigenpairs $(\widehat{\lambda}_i, \widehat{v}_i)$ in the interval \mathcal{I} ;
-

A few remarks are in order:

- In practice, we never need to form the matrix \widehat{A}_j at step 6 explicitly. We can assume that the only operation that is required by EIGSOL is the matrix-vector product $y := \widehat{A}_j x$.
- At step 7, the computation of the lowest eigenpair $(\widehat{\lambda}_{j+1}, \widehat{v}_{j+1})$ of \widehat{A}_j can be accelerated by warm starting the EIGSOL with the lowest unconverged eigenvectors of \widehat{A}_{j-1} . This is possible for most iterative eigensolvers, such as TRLAN [20] and ARPACK [9].
- At step 8, an ideal validation method is to use the inertias of the shifted matrix $A - \lambda_{\text{upper}} I$. However, computation of the inertias is a prohibitive cost for large matrices. An empirical validation is to monitor the lowest eigenvalue $\widehat{\lambda}_{j+1}$ of \widehat{A}_j . All eigenpairs in the interval \mathcal{I} are considered to be found when $\widehat{\lambda}_{j+1}$ is outside the interval \mathcal{I} .

5 Numerical experiments

In this section, we first use synthetic examples to verify the sharpness of the upper bounds (3.10) and (3.24) on the loss of orthogonality and the symmetric backward error norm of the EED procedure under the choice (4.5) of the shifts σ_j . We present the cases where improper choices of the shifts σ_j may lead to numerical instability of the EED procedure. Then we demonstrate the numerical stability of the EED procedure for a set of large sparse symmetric matrices arising from applications.

We use TRLAN as the eigensolver. TRLAN is a C implementation of the thick-restart Lanczos method with adaptive sizes of the projection subspace [20, 22, 23]. The convergence criterion of an approximate eigenpair $(\widehat{\lambda}_{j+1}, \widehat{v}_{j+1})$ is the residual norm satisfying

$$\|\eta_{j+1}\|_2 = \|\widehat{A}_j \widehat{v}_{j+1} - \widehat{\lambda}_{j+1} \widehat{v}_{j+1}\|_2 < \text{tol} \cdot \mathbf{Anorm},$$

where tol is a user-specified tolerance and \mathbf{Anorm} is a 2-norm estimate of A computed by TRLAN. The starting vector is a random vector.

Example 5.1. In this example, we demonstrate the sharpness of the upper bounds (3.10) and (3.24) on the loss of orthogonality and the symmetric backward error norm with the choice (4.5) of the shifts σ_j .

We consider a diagonal matrix A with diagonal elements

$$a_{kk} = \begin{cases} \frac{1}{2} d_k, & \text{if } 1 \leq k \leq n/2, \\ \frac{1}{2}(1 + d_{k-n/2}), & \text{if } n/2 < k \leq n, \end{cases}$$

where $d_k = 10^{-5(1 - \frac{k-1}{n/2-1})}$ and the matrix size $n = 500$. The spectrum range of A is $(0, 1]$. The eigenvalues of A are clustered around 0 and 0.5. We are interested in computing the $n_e = 65$ eigenvalues in the interval $\mathcal{I} = [0, 10^{-4}]$. The computed 2-norm of A is $\mathbf{Anorm} = 1.00$.

To closely observe the convergence, TRLAN is slightly modified so that the convergence test is performed at each Lanczos iteration. The maximal dimension m of the projection subspace is set to be 40.

Numerical results of TRLAN with the EED procedure for computing all the n_e eigenvalues in the interval \mathcal{I} are summarized in Table 1, where the 4th column is the loss of orthogonality ω_{n_e} , the 5th column is the upper bound (3.10) of ω_{n_e} , the 6th column is the residual norm $\|R_{n_e}\|_F$ and

Table 1: Numerical stability of TRLan with EED for different tolerances tol (Example 5.1)

tol	μ	γ_g	ω_{n_e}	bound (3.10)	$\ R_{n_e}\ _F$	bound (3.24)
10^{-6}	1.00	1.00	$2.37 \cdot 10^{-6}$	$1.59 \cdot 10^{-5}$	$7.87 \cdot 10^{-6}$	$2.24 \cdot 10^{-5}$
10^{-8}	1.00	1.00	$1.78 \cdot 10^{-8}$	$1.58 \cdot 10^{-7}$	$7.95 \cdot 10^{-8}$	$2.24 \cdot 10^{-7}$
10^{-10}	1.00	1.00	$1.82 \cdot 10^{-10}$	$1.58 \cdot 10^{-9}$	$7.94 \cdot 10^{-10}$	$2.24 \cdot 10^{-9}$

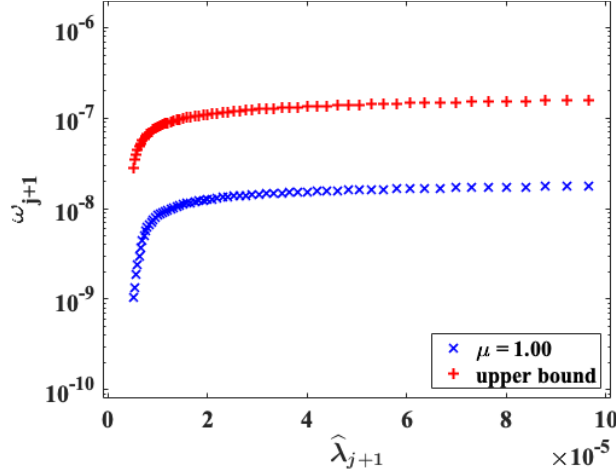


Figure 2: The loss of orthogonality ω_{j+1} and the upper bound (3.10) of ω_{j+1} against the computed eigenvalues $\hat{\lambda}_{j+1}$ for $2 \leq j+1 \leq n_e$, $tol = 10^{-8}$ (Example 5.1).

the 7th column is the upper bound (3.24) of δ_{n_e} . Note that here we use the quantities δ_{n_e} and $\|R_{n_e}\|_F$ interchangeably as discussed in Remark 3.2.

From Table 1, we observe that with the choice (4.5) of the shifts σ_j , $\gamma_g^{-1} \mathbf{Anorm} \approx 1$ and $\tau_g \approx 1$. Therefore, the conditions (3.37) of the spectral gap γ_j and the shift-gap ratio τ_j for the backward stability are satisfied. Consequently, the loss of orthogonality of the computed eigenvectors is $\omega_{n_e} = O(tol)$ and the symmetric backward error norm of the computed eigenpairs $(\hat{\Lambda}_{n_e}, \hat{V}_{n_e})$ is $\delta_{n_e} = O(tol \cdot \mathbf{Anorm})$. In addition, we observe that the upper bounds (3.10) and (3.24) of ω_{n_e} and δ_{n_e} are tight within an order of magnitude.

Example 5.2. In this example we illustrate that improperly chosen shifts σ_j may lead to instability of the EED procedure.

In Remark 3.3, we stated that if the shifts σ_j are chosen such that the spectral gaps γ_j are too small, i.e., $\gamma_j \ll \mathbf{Anorm}$, then the loss of orthogonality of the computed eigenvectors could be amplified by a factor of $\gamma_j^{-1} \cdot \mathbf{Anorm}$. Here is an example using the same diagonal matrix A in Example 5.1. The combination of TRLan and EED is used to compute the $n_e = 65$ eigenvalues in the interval $\mathcal{I} = [0, 10^{-4}]$. Let us set the shifts $\sigma_j = \mu - \hat{\lambda}_j$ with $\mu = 2 \cdot 10^{-4}$, which is much smaller than the recommended value of $\mu = \hat{\lambda}_1 + \|A\|_2 \approx 1.00$. Numerical results are summarized in Table 2, where the tolerance $tol = 10^{-8}$ for TRLan. We observe that $\gamma_j = O(\gamma_g) \ll \mathbf{Anorm}$, and the loss of orthogonality of the computed eigenvectors is indeed amplified by a factor of $\gamma_g^{-1} \cdot \mathbf{Anorm}$. We note that since $\tau_j = O(1)$, the symmetric backward error norms $\delta_{n_e} = O(tol \cdot \mathbf{Anorm})$.

In Remark 3.3, we also stated that if the shifts σ_j are chosen such that the shift-gap ratios τ_j are too large, then the symmetric backward error norm δ_j could be amplified by a factor of τ_j . Here is an example. We flip the sign of the diagonal elements of A defined in Example 5.1, and set

Table 2: Instability of TRLan with EED when the spectral gaps $\gamma_j = O(\gamma_g)$ are too small.

tol	μ	γ_g	ω_{n_e}	bound (3.10)	$\ R_{n_e}\ _F$	bound (3.24)
10^{-6}	$2 \cdot 10^{-4}$	10^{-4}	$8.26 \cdot 10^{-3}$	$1.79 \cdot 10^{-1}$	$8.00 \cdot 10^{-6}$	$3.29 \cdot 10^{-5}$
10^{-8}	$2 \cdot 10^{-4}$	10^{-4}	$8.28 \cdot 10^{-5}$	$1.53 \cdot 10^{-3}$	$7.96 \cdot 10^{-8}$	$3.22 \cdot 10^{-7}$
10^{-10}	$2 \cdot 10^{-4}$	10^{-4}	$8.27 \cdot 10^{-7}$	$1.52 \cdot 10^{-5}$	$7.95 \cdot 10^{-10}$	$3.22 \cdot 10^{-9}$

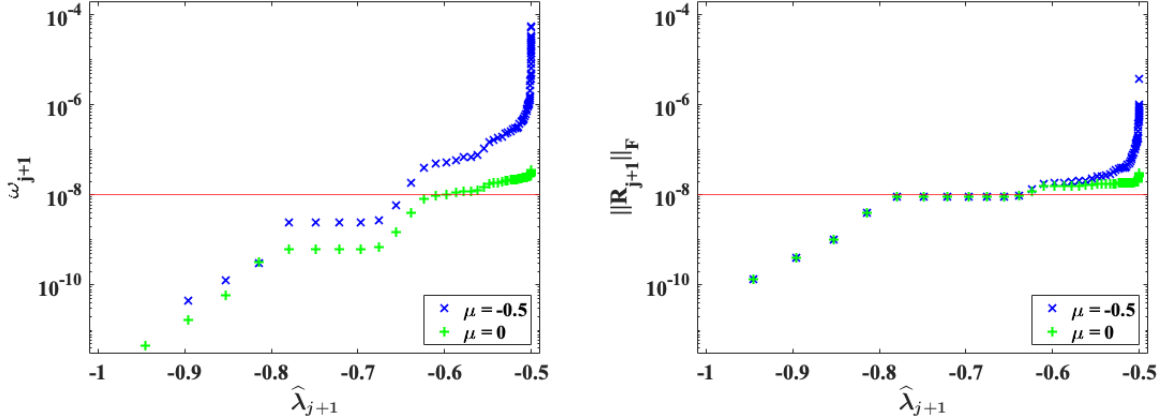


Figure 3: The loss of orthogonality ω_{j+1} (left) and the residual norm $\|R_{j+1}\|_F$ (right) against the computed eigenvalues $\hat{\lambda}_{j+1}$ for $2 \leq j+1 \leq n_e$. The red lines are tol (left) and $tol \cdot \mathbf{Anorm}$ (right).

$n = 200$. We compute $n_e = 74$ eigenvalues in the interval $\mathcal{I} = [-1.0, -0.5001]$ using TRLan with EED procedure. The computed 2-norm of A is $\mathbf{Anorm} = 1.00$.

Instead of the choice (4.5) for the shifts σ_j , we set $\sigma_j = \mu - \hat{\lambda}_j$ with $\mu = -0.5$. The blue \times -lines in Figure 3 are the loss of orthogonality and the residual norms for the computed eigenpairs $(\hat{\lambda}_{j+1}, \hat{v}_{j+1})$ for $2 \leq j+1 \leq n_e$. As we observe that for the first 6 computed eigenvalues in the subinterval $[-1.0, -0.75]$ of \mathcal{I} , since the spectral gap $\gamma_j \geq 0.25$ and the shift-gap ratio $\tau_j \leq 2$, the computed eigenpairs are backward stable with $\omega_6 = 2.48 \cdot 10^{-9} = O(tol)$ and $\|R_6\|_F = 9.05 \cdot 10^{-9} = O(tol \cdot \mathbf{Anorm})$. However, for the computed eigenvalues in the subinterval $[-0.75, -0.5001]$ of \mathcal{I} , the computed eigenpairs are not backward stable due to the facts that the spectral gaps γ_j become small, $\gamma_j \approx 1.03 \cdot 10^{-4}$, and the shift-gap ratios τ_j grows up to $\tau_j \approx 4.86 \cdot 10^3$. Consequently, the loss of orthogonality ω_{n_e} and the residual norm $\|R_{n_e}\|_F$ are increased by a factor of up to 10^3 , respectively. The stability are restored if the shifts are chosen according to the recommendation (4.5) as shown by the green $+$ -lines in Figure 3.

Example 5.3. In this example, we demonstrate the numerical stability of TRLan with the EED procedure for a set of large sparse symmetric matrices from applications.

The statistics of the matrices are summarized in Table 3, where n is the size of the matrix, nnz is the number of nonzero entries of the matrix, $[\lambda_{\min}, \lambda_{\max}]$ is the spectrum range, and n_e is the number of eigenvalues in the interval $\mathcal{I} = [\lambda_{\text{low}}, \lambda_{\text{upper}}]$. The quantities n_e are calculated by computing the inertias of the shifted matrices $A - \lambda_{\text{upper}}I$. The **Laplacian** is the negative 2D Laplacian on a 200-by-200 grids with Dirichlet boundary condition [16]. The **worms20** is the graph Laplacian worms20_10NN in machine learning datasets [4]. The **Si0**, **Si34H36**, **Ge87H76** and **Ge99H100** are Hamiltonian matrices from PARSEC collection [4].

We run TRLan with a maximal number m of Lanczos vectors to compute the lowest eigenpairs of the matrix \hat{A}_j . The convergence test is performed at each restart of TRLan. All the converged eigenvalues in the interval \mathcal{I} are shifted by EED. Meanwhile, we also keep a maximal number m_0

Table 3: Statistics of the test matrices.

matrix	n	nnz	$[\lambda_{\min}, \lambda_{\max}]$	$[\lambda_{\text{low}}, \lambda_{\text{upper}}]$	n_e
Laplacian	40,000	199,200	[0, 7.9995]	[0, 0.07]	205
worms20	20,055	260,881	[0, 6.0450]	[0, 0.05]	289
Si0	33,401	1,317,655	[-1.6745, 84.3139]	[-1.7, 2.0]	182
Si34H36	97,569	5,156,379	[-1.1586, 42.9396]	[-1.2, 0.4]	310
Ge87H76	112,985	7,892,195	[-1.214, 32.764]	[-1.3, -0.0053]	318
Ge99H100	112,985	8,451,395	[-1.226, 32.703]	[-1.3, -0.0096]	372

Table 4: Numerical results of TRLED.

matrix	\hat{n}_e	j_{\max}	$\omega_{\hat{n}_e}$	$\ R_{\hat{n}_e}\ _{\text{F}}/\text{Anorm}$	CPU time (sec.)	
					TRLED	TRLan
Laplacian	205	60	$1.93 \cdot 10^{-8}$	$6.33 \cdot 10^{-8}$	66.5	86.0
worms20	289	86	$2.63 \cdot 10^{-8}$	$7.24 \cdot 10^{-8}$	57.3	74.8
Si0	182	41	$2.33 \cdot 10^{-8}$	$4.71 \cdot 10^{-8}$	42.4	47.1
Si34H36	310	72	$3.41 \cdot 10^{-8}$	$7.50 \cdot 10^{-8}$	309.9	310.4
Ge87H76	318	66	$4.08 \cdot 10^{-8}$	$8.50 \cdot 10^{-8}$	388.7	421.0
Ge99H100	372	74	$3.65 \cdot 10^{-8}$	$7.63 \cdot 10^{-8}$	501.1	533.4

of the lowest unconverged eigenvectors as the starting vectors of TRLan for the matrix \hat{A}_{j+1} . All the eigenvalues in \mathcal{I} are assumed to be computed when the lowest converged eigenvalue is outside the interval \mathcal{I} . This combination of TRLan is referred to as TRLED.

TRLED is compiled using the `icc` compiler (version 2021.1) with the optimization flag `-O2`, and linked to BLAS and LAPACK available in Intel Math Kernel Library (version 2021.1.1). The experiments are conducted on a MacBook with 1.6 GHz Intel Core i5 CPU and 8GB of RAM.

For numerical experiments, we set the maximal number of Lanczos vectors $m = 150$. When starting TRLED for \hat{A}_{j+1} , the maximal number of the starting vectors is $m_0 = 75$. The convergence tolerance for the residual norm was set to $tol = 10^{-8}$ as a common practice for solving large scale eigenvalue problems with double precision; see for example [11].

Numerical results of TRLED are summarized in Table 4, where the 2nd column is the number \hat{n}_e of the computed eigenpairs $(\hat{\lambda}_i, \hat{x}_i)$ in the interval \mathcal{I} , the 3rd column is the number j_{\max} of steps of EED performed, the 4th column is the loss of orthogonality $\omega_{\hat{n}_e}$, and the 5th column is the relative residual norm $\|R_{\hat{n}_e}\|_{\text{F}}/\text{Anorm}$ of the computed eigenpairs $(\hat{\Lambda}_{n_e}, \hat{V}_{n_e})$. From the quantities n_e in Table 3 and \hat{n}_e in Table 4, we see that for all test matrices the eigenvalues in the prescribed intervals \mathcal{I} are successfully computed with the desired backward stability.

The left plot of Figure 4 is a profile of the number of converged eigenvalues at each external deflation of a total of 74 EEDs for the matrix Ge99H100. The right plot of Figure 4 shows the relative residual norms of all 372 computed eigenpairs in the interval. We observe that a large number of converged eigenvalues are deflated and shifted away at some EED steps.

To examine whether the multiple explicit external deflations lead to a significant increase in execution time, in the 6th and 7th columns of Table 4, we record the CPU time of TRLED and TRLan for computing all eigenvalues in the same intervals. For TRLan, we set the maximal number of Lanczos vectors to $n_e + 150$. The restart scheme with `restart=1` is used. TRLan is compiled and executed under the same setting as TRLED. We observe comparable execution time of TRLED and TRLan. In fact, TRLED is slightly faster. We think this might be due to the facts that TRLED

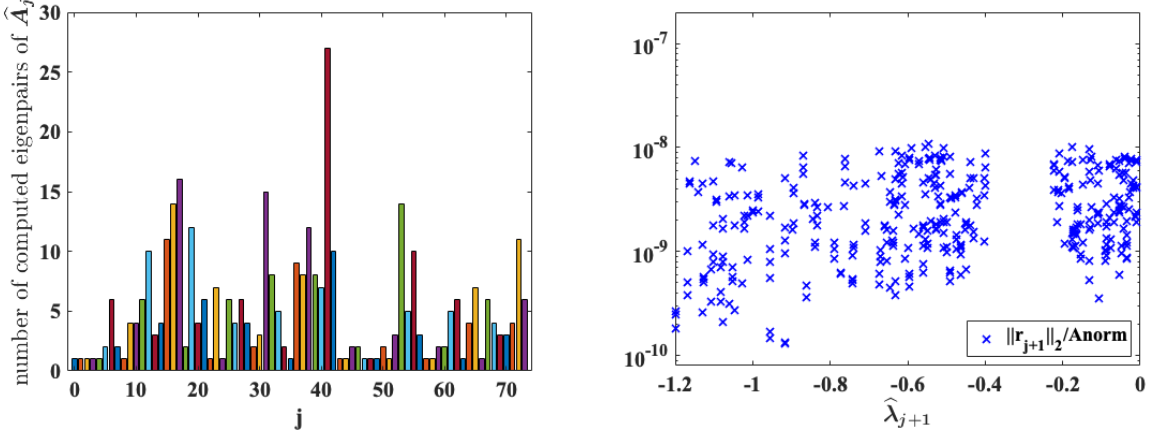


Figure 4: The number of deflated eigenpairs at each EED for the matrix Ge99H100 (left). The relative residual norms of 372 computed eigenpairs (right).

uses fewer Lanczos vectors, which compensates the cost of the matrix-vector products $y := \widehat{A}_j x$ and the warm start with those unconverged eigenvectors from the previous deflated matrix \widehat{A}_{j-1} . These are subjects of future study.

6 Concluding remarks

Based on the governing equations of the EED procedure in finite precision arithmetic, we derived the upper bounds on the loss of the orthogonality of the computed eigenvectors and the symmetric backward error norm of the computed eigenpairs in terms of two key quantities, namely the spectral gaps and the shift-gap ratios. Consequently, we revealed the required conditions of these two key quantities for the backward stability of the EED procedure. We present a practical strategy on the dynamically selection of the shifts such that the spectral gaps and the shift-gap ratios satisfy the required conditions.

There are a number of topics that can be explored further. One of them is the acceleration effect of the warm starting the EIGSOL with the unconverged eigenvectors of \widehat{A}_{j-1} for computing of the lowest eigenpairs of \widehat{A}_j . Another one is how to efficiently perform the matrix-vector products $y := \widehat{A}_j x$ in EIGSOL by exploiting the sparse plus low rank structure of the matrix \widehat{A}_j . Communication-avoid algorithms for sparse-plus-low-rank matrix-vector products can be found in [10, 7]. A preliminary numerical study for high performance computing is reported in [21].

References

- [1] Z. Bai, J. Demmel, J. Dongarra, A. Ruhe, and H. van der Vorst. *Templates for the Solution of Algebraic Eigenvalue Problems: A Practical Guide*. SIAM, Philadelphia, PA, 2000.
- [2] Z. Bai, R.-C. Li, and W. Lin. Linear response eigenvalue problem solved by extended locally optimal preconditioned conjugate gradient methods. *Sci. China Math.*, 259:1443–1460, 2016.
- [3] P.-Y. Chen, B. Zhang, and M. Al Hasan. Incremental eigenpair computation for graph laplacian matrices: theory and applications. *Social Network Analysis and Mining*, 8(1):4, 2018.

- [4] T. Davis and Y. Hu. The University of Florida sparse matrix collection. *ACM Trans. Math. Software (TOMS)*, 38(1):1–25, 2011.
- [5] D. Higham and N. Higham. Structured backward error and condition of generalized eigenvalue problems. *SIAM J. Mat. Anal. Appl.*, 20(2):493–512, 1998.
- [6] H. Hotelling. Analysis of a complex of statistical variables into principal components. *J. of Educational Psychology*, 24(6):417, 1933.
- [7] N. Knight, E. Carson, and J. Demmel. Exploiting data sparsity in parallel matrix powers computations. In *the proceedings of the international conference on parallel processing and applied mathematics (PPAM)*, 2014.
- [8] R. Lehoucq and D. Sorensen. Deflation techniques for an implicitly restarted Arnoldi iteration. *SIAM J. Matrix Anal. Appl.*, 17(4):789–821, 1996.
- [9] R. Lehoucq, D. Sorensen, and C. Yang. *ARPACK Users’ Guide: Solution of Large-Scale Eigenvalue Problems with Implicitly Restarted Arnoldi Methods*. SIAM, Philadelphia, PA, 1998.
- [10] C. Leiserson, S. Rao, and S. Toledo. Efficient out-of-core algorithms for linear relaxation using blocking covers. *J. Comput. Syst. Sci. Int.*, 54:332–344, 1997.
- [11] R. Li, Y. Xi, E. Vecharynskio, C. Yang, and Y. Saad. A thick-restart Lanczos algorithm with polynomial filtering for Hermitian eigenvalue problems. *SIAM J. Sci. Comput.*, 38:A2512–A2534, 2016.
- [12] J. Money and Q. Ye. Algorithm 845: EIGIFP: a MATLAB program for solving large symmetric generalized eigenvalue problems. *ACM Trans. Math. Software (TOMS)*, 31(2):270–279, 2005.
- [13] B. N. Parlett. *The Symmetric Eigenvalue Problem*. SIAM, Philadelphia, PA, 1998.
- [14] Y. Saad. Numerical solution of large nonsymmetric eigenvalue problems. *Comput. Phys. Commun.*, 53(1-3):71–90, 1989.
- [15] Y. Saad. *Numerical Methods for Large Eigenvalue Problems: revised edition*, volume 66. SIAM, Philadelphia, PA, 2011.
- [16] B. Smith and A. Knyazev. *Laplacian in 1D, 2D or 3D*, 2015 (accessed March 24, 2020). <https://www.mathworks.com/matlabcentral/fileexchange/27279-laplacian-in-1d-2d-or-3d>.
- [17] Danny C Sorensen. Implicit application of polynomial filters in a k -step Arnoldi method. *SIAM J. Matrix. Anal. Appl.*, 13(1):357–385, 1992.
- [18] J.-G. Sun. A note on backward perturbations for the Hermitian eigenvalue problem. *BIT Numer. Math.*, 35(3):385–393, 1995.
- [19] J. H. Wilkinson. *The algebraic eigenvalue problem*. Clarendon Press, Oxford, 1965.
- [20] K. Wu and H. Simon. Thick-restart Lanczos method for large symmetric eigenvalue problems. *SIAM J. Matrix Anal. Appl.*, 22(2):602–616, 2000.

- [21] I. Yamazaki, Z. Bai, D. Lu, and J. Dongarra. Matrix powers kernels for thick-restart Lanczos with explicit external deflation. In *2019 IEEE International Parallel Distributed Processing Symposium (IPDPS)*, pages 472–481. IEEE, 2019.
- [22] I. Yamazaki, Z. Bai, H. Simon, L.-W. Wang, and K. Wu. Adaptive projection subspace dimension for the thick-restart Lanczos method. *ACM Trans. Math. Software (TOMS)*, 37(3):27, 2010.
- [23] I. Yamazaki, K. Wu, and H. Simon. nu-TRLan User Guide. Technical report, LBNL-1288E, 2008. Software <https://codeforge.lbl.gov/projects/trlan/>.